Near-field optical spectroscopy of individual surface-plasmon modes in colloid clusters

V. A. Markel*
Department of Physics, New Mexico State University, Las Cruces, New Mexico 88003
and Institute of Automation and Electrometry, Siberian Branch of RAS, 630090, Novosibirsk, Russia

V. M. Shalaev
Department of Physics, New Mexico State University, Las Cruces, New Mexico 88003

P. Zhang, W. Huynh, L. Tay, T. L. Haslett, and M. Moskovits
Department of Chemistry, University of Toronto, and Photonics Research Ontario, Toronto, Canada M5S 3H6
(Received 2 October 1998)

Local spectra of self-affine clusters of silver colloid particles recorded with subwavelength resolution by near-field spectroscopy are reported. Spectra were also simulated computationally. The observed and calculated near-field spectra consist of several resonances with highly location-dependent frequencies. The most highly resolved of these resonances correspond to individual surface plasmon (SP) normal modes. All of these features are only observable in the near field. Both theory and experiment also show that when excited by light in the SP region of the spectrum, the field-intensity distribution in the near field is very heterogeneous with most of the excitation concentrated in "hot spots" on the cluster surface that are strongly excitation-wavelength dependent. This field-intensity localization provides a rationale for recently reported surface-enhanced Raman enhancements in excess of 10^{10}. [S0163-1829(99)01115-7]

INTRODUCTION

Disordered systems manifest optical properties that are both fascinating and unusual.[1] Specifically, coupled oscillators distributed on a fractal object, that is, an object possessing dilational symmetry, are predicted to possess normal modes of oscillation in which the excitation is, in general, not distributed uniformly over the body of the fractal but is localized in "hot spots," often much smaller than the wavelength. Consequently, when one or several of these normal modes is excited, most of the volume [or for two-dimensional (2D) fractals, the area] of the fractal remains almost unexcited while the portion of the fractal within the hot spots carries the full excitation that, for a nonfractal object, would have been distributed over the entire object.[2] The locations of the hot spots are predicted to depend strongly on the sample geometry and on the excitation wavelength and polarization. The hot spots ultimately result from the dilational symmetry, causing the electromagnetic excitations of fractals to be neither describable as conventional surface-plasmon waves (polaritons) nor as independent localized surface plasmons. For self-affine films such as those described below, i.e., for films with a fractal geometry such that the dilational invariance in the plane and normal to average plane of the surface are different, the localization results from the fact that the surface does not possess lateral translational invariance and, therefore, laterally propagating running waves cannot be transmitted on it. This is a consequence of the fact that running waves are not eigenfunctions of the dilation symmetry operator that characterizes self-affine surfaces.

These conclusions are pertinent to surface-enhanced Raman scattering (SERS) and other surface-enhanced optical effects. Many systems that show surface-enhanced optical effects are fractal clusters or fractal surfaces. These include rough metal surfaces generated by condensing metal on a cold surface and aggregates of colloidal metal particles, often consisting of tens of thousands of particles. Such fractal systems should, then, manifest the above-mentioned effects when illuminated with light in an appropriate wavelength range, which in this case would be the region of the surface plasmon resonance (SP)—narrow resonances involving collective motions of the conduction electrons. For particles much smaller than the excitation wavelength, the SP resonances are almost entirely dipolar. Aggregating such particles allows their dipoles to couple, thereby converting the set of dipolar resonances of the individual particles into normal modes of excitation that embrace the aggregate, or very large portions of it. It is known that at the SP resonance, the average electromagnetic field intensities at the surface of even the individual particles of metals such as silver or gold, can be greatly enhanced.[3] When coupled, these enhancements can increase further, and when localized at hot spots as a result of the fractal geometry of the aggregate, the enhancements are predicted to become enormous.[1,2] This might explain, for example, some of the recent reports of Kneipp *et al.*[4] of SERS enhancements in excess of 10^{10} in systems so dilute in adsorbate that the SERS being measured originates from individual molecules. The enhancement of localized, nonlinear effects should result in even more remarkable enhancements. For example, third-order nonlinear processes are predicted to be enhanced by factors of the order of 10^{15}.[5]

The optical theory of fractals also predicts that the absorption spectrum of a large enough fractal aggregate will be a very broad, inhomogeneous envelope of, hitherto unobserved, overlapping homogeneous spectral lines each due to an individual normal mode. The broad envelope is expected to approach a "universal curve" for a given fractal type.

Because of the the above-mentioned field localization, the local spectrum of a subwavelength portion of a fractal cluster will reflect the participation of that part of the fractal in its various normal modes, yielding a structured spectrum in which some of the peaks would correspond to the homogeneous spectra of individual normal modes.

In this paper we present the first near-field spectra of a self-affine fractal surface prepared by collapsing colloidal silver-particle aggregates gravitationally. We also report a parallel theoretical study in which near-field excitation spectra are computed at various points above model surfaces that simulate those used in the experiment. Our results strikingly illustrate the field localization and the presence of individual normal modes in the near-field spectra of fractal surfaces. Such results are observable only in the near-field since in the far field one probes spectroscopic contributions from many subwavelength regions of the object, thereby obtaining the inhomogeneous, average "envelope" spectrum. Preliminary near-field imaging of fractal surfaces was previously reported.[6] Near-field spectra of *individual* colloidal particles have also been reported.[7]

EXPERIMENTAL

Experiments were carried out using a near-field optical microscope consisting of a piezoelectric scanning tube mounted coaxially on a Burleigh inchworm linear motor used for coarse approach. The sample, which is deposited on a piece of a Pyrex cover slide, is mounted with index-matching fluid on a microdovetail attenuated total reflection (ATR) prism. It is excited by the evanescent wave of a laser beam totally internally reflected inside the ATR prism. The light beam is conducted to the entrance surface of the prism using an optical fiber, which is fixed to the scanning tube with a collet so designed that the illumination of the sample does not change as the sample is rastered. The probe tip consists of a single-mode optical fiber sharpened by drawing at constant tension while being locally heated in the microscopic arc discharge of a commercial fiber splicer.[8] Height regulation was achieved by using a modified version of shear-force microscopy.[9] The fiber tip is attached to a piezoelectric bimorph that sets it vibrating at its resonant frequency. The vibrational amplitude is measured using lock-in detection of the time-dependent signal resulting from the shadow of the tip cast on a two-sector photodetector. The tip was inclined at approximately 45° to the surface, approximating, thereby, atomic-force microscopy in the so-called tapping mode. Experiments were run at a height of approximately 25 nm above the surface. Recording the voltage to the z control of the piezoelectric scanning tube as a function of lateral position, so as to keep the vibrational amplitude of the tip constant, produces an approximate topographic image of the sample, which is recorded simultaneously with the near-field optical image. (One should clarify at this point what is meant by "height" in the present context. The tip is not a point tip. Additionally, the surface is not planar but has a complicated geometry. Consequently, what is measured will not correspond, in general, to the shortest distance between the lowest-most point on the tip and the surface. Operationally, one assumes that at the height at which the tip amplitude just vanishes, the tip is in contact with the surface. This procedure damages the tip and can only be performed at the end of an experiment. However, we noted that the amplitude-height curve for all of the tips measured had approximately the same form, hence we could assume that reducing the tip amplitude by a certain fraction of its maximum amplitude placed the tip approximately at the same operational "height" above the surface). Near-field excitation spectra were obtained by scanning the wavelength of the illumination laser (which was either a dye or a Ti:sapphire laser) while keeping the fiber tip fixed (within the limitations imposed by thermal motion) over a spot on the sample.

Self-affine fractal surfaces were prepared by gravitationally depositing fractal aggregates of colloidal silver particles (particle diameter ~20 nm) out of solution onto Pyrex microscope cover slides as described previously.[6,10] In solution the fractal clusters are known to be self-similar fractals with a Hausdorff dimension of ~1.8.[11] Upon deposition, the clusters become compacted in the vertical direction while retaining, more or less, their original fractal character in the two horizontal directions, thereby becoming self-affine. This is confirmed by recent calculations.[12] The coarse structure of the samples was imaged using confocal optical microscopy.

COMPUTATIONAL DETAILS

Self-affine surfaces and films are characterized by a height-height correlation function, which obeys a power-law dependence of the form

$$g(r)=\langle[z(\mathbf{R})-z(\mathbf{R}+\mathbf{r})]^2\rangle \propto r^{2(3-D)},$$

where $\mathbf{r}$ and $\mathbf{R}$ are position vectors lying in the xy plane, $z(\mathbf{r})$ is the height of the surface at $\mathbf{r}=(x,y)$, and D is the fractal dimension. In random but, on average, homogeneous surfaces, this function decays exponentially, and becomes zero for distances larger than a characteristic correlation length, l_c, which is a few times greater than the size of the smallest roughness features. The above power-law dependence is applicable over a size scale ranging from the smallest roughness features to some large, possibly macroscopic, length.

Electric-field distributions and the wavelength dependence of the field strength at various spots near a computer-generated fractal surface were computed by placing cube-shaped monomers on a cubic lattice to produce three-dimensional cluster-cluster aggregates with fractal dimension $D=1.8$.[13] The aggregate was projected onto a plane so that no empty spaces were left underneath any given monomers; however, no lateral restructuring was allowed. The height-height correlation function calculated for the resulting film showed it to be self-affine with $D_H \cong 2.6$. This process adequately simulates the experimental strategy used to produce self-affine surfaces.

Each elementary cube was assumed to be 8 nm, in the same size range as the silver-colloid particles used in the experiment, which had a mean diameter of ~20 nm. Computations were carried out on films with $N=10{,}000$ and $=2{,}500$ monomers, corresponding to linear dimensions in the xy plane of the order of, or greater than the incident wavelength. The computed films were typically $1500 \times 1200\,\text{nm}^2$ with a maximum height of approximately 120 nm. Calculations were carried out in the spectral range $\lambda = 540$ to 1000 nm. The exponential decay constant for the

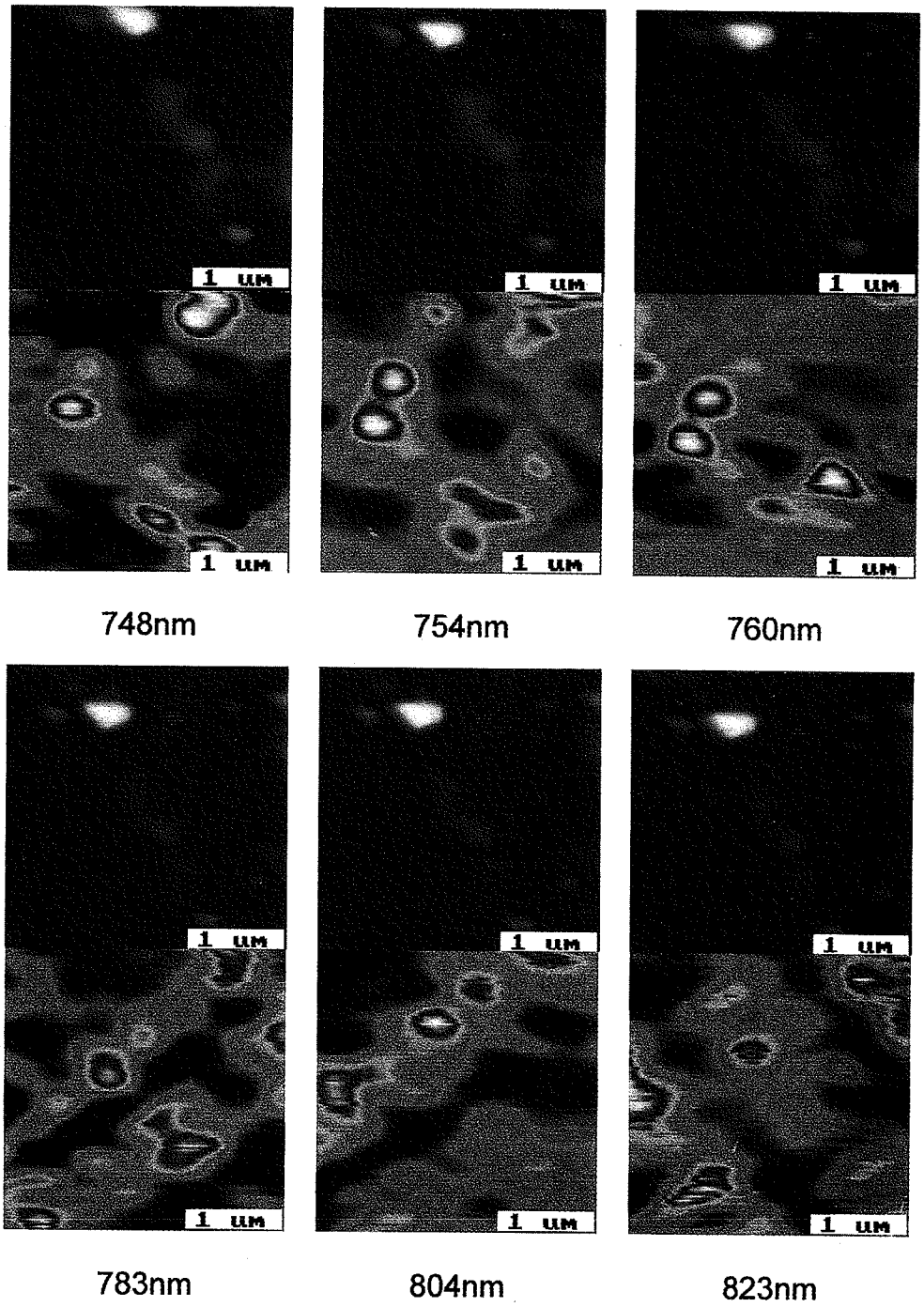

FIG. 1. (Color) Near-field images (false color) and simultaneously recorded topographic images (thermal colors) obtained by exciting a silver-colloid cluster deposited out of solution onto a Pyrex surface with a Ti:sapphire laser. The images were recorded with a sharpened fiber tip scanning 25 nm above the surface. The false color range corresponds to approximately a factor of 4, with dark blue indicating the low-intensity spots and yellow the high-intensity regions. The average optical intensity in the near-field images is approximately 100-fold higher than the signal from a clean Pyrex control surface. The height range in the topographic images is approximately 90 nm.

evanescent field is $\sim 2.5\ \lambda$, i.e., much greater than the film's height (for a refractive index of 1.53 and angle of incidence of $\pi/4$). Hence, the film is being excited by an almost homogeneous field of strength more or less equivalent to what would be experienced were the film excited by the same laser from the optically rarer medium.

The clusters were assumed to be excited by the evanescent field that penetrates the space above the ATR prism. Each monomer of the film was considered to be an elementary dipole possessing a scalar polarizability α, whose value can be determined from expressions appropriate to the size and shape of the monomer, using published optical constants of silver (or any other material). This approach is equivalent to the discretization of the exact Maxwell equations.[14] The elementary dipoles interact with the incident evanescent fields and with each other via the dipole-radiation fields established self consistently by the radiating dipoles. Such a system can be described by a system of self-consistent linear equations, known as the coupled dipole equations (CDE),[15] whose (numerical) solutions express the amplitudes of all of

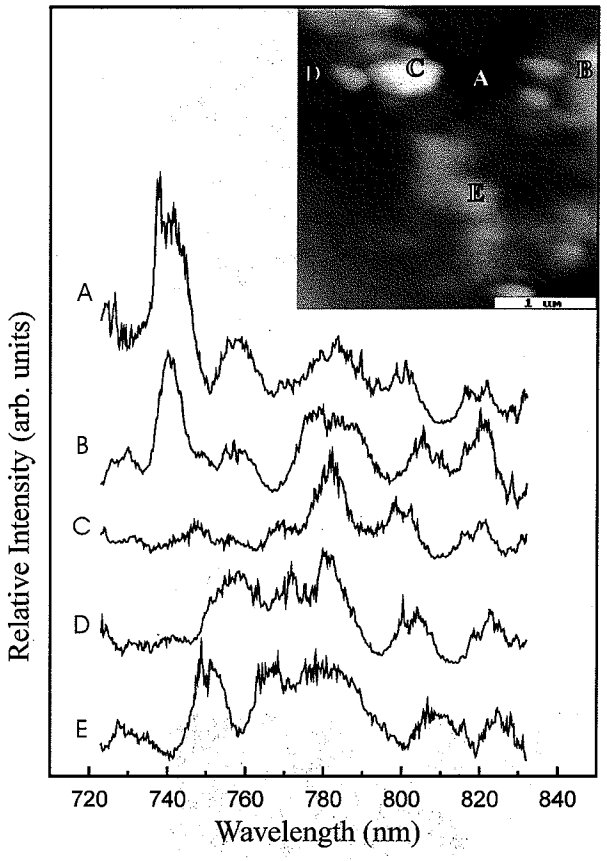

FIG. 2. Near-field spectra collected by placing the near-field fiber probe 25 nm above the surface of the self-affine silver cluster and scanning a Ti:sapphire laser over the wavelength range indicated. The letters at the leftmost edge of each spectrum correspond to the locations indicated by letters on the topographic image.

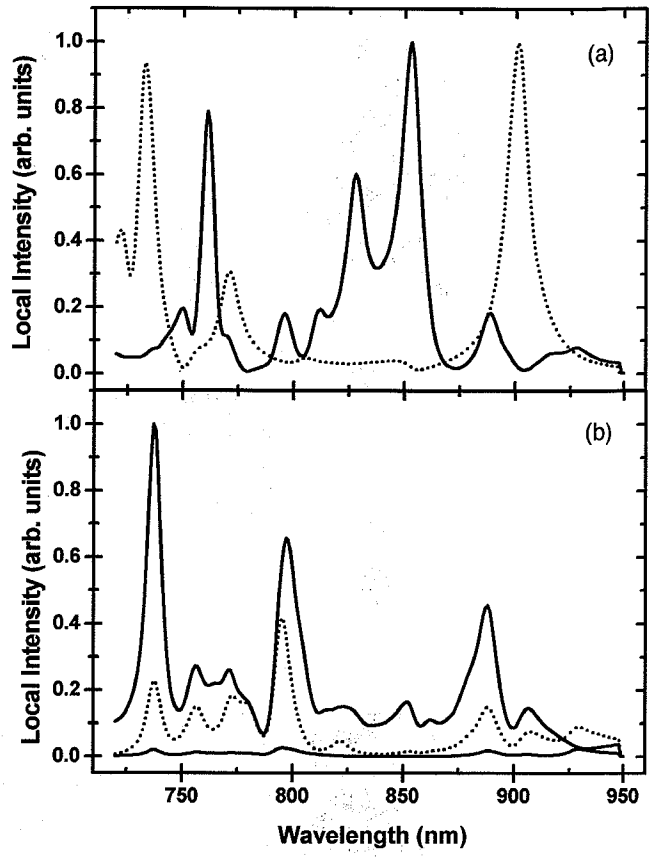

FIG. 3. Near-field spectra (i.e., the square modulus of the field calculated at a point above a simulated self-affine silver cluster) calculated as a function of wavelength at several locations above the cluster. (a) Spectra calculated at a height 10 nm above the surface for two points separated by a horizontal distance of 580 nm. The two spectra are normalized to unity. (b) A series of spectra calculated at three heights above the surface ($h = 10$, 20, and 40 nm in order of decreasing intensity) for a third location on the simulated silver cluster approximately 72 nm from the point that generates the solid curve in plot A.

the elementary dipoles and of the electromagnetic fields at any point in space, inside or above the surface, within the dipole approximation. The CDE were solved by the conjugate gradient method for $N = 10000$ and by the LU expansion for $N = 2500$ using a Hewlett-Packard EXEMPLAR SPP-2000 supercomputer.

RESULTS AND DISCUSSION

The self-affine samples used in the experiments consist of a large number of well-separated aggregates of colloidal silver particles, each aggregate consisting, on average, of several tens of thousands of silver colloid particles arranged so as to form self-affine objects. Typical near-field images measured at the surface of such clusters are shown in Fig. 1. Shown above each near-field image is a topographic image obtained using shear-force microscopy modified as described above. Near-field optical (and topographic) images in various other wavelength ranges were also obtained. All of those measurements tell essentially the same story. (i) The excitation of the surface is localized in regions often smaller than the wavelength. (ii) The near-field images are very wavelength dependent—even a rather small wavelength shift (c.f. Fig. 1) can result in very different near-field images. (iii) The images are reproducible; returning to the same excitation wavelength produces the very same near-field image even after several hours. (iv) The images are definitely due to the presence of the self-affine silver surface. Control experiments indicate that in the absence of silver the near-field image is structure-free and the average measured intensity is approximately 100-fold lower, similar to previously reported images using Ar^+ laser excitation.[6]

The measured near-field spectra are even more striking. Figure 2 shows five typical near-field spectra. The locations on the silver surface at which each spectrum was taken are shown in the topographic image at the upper right-hand corner of the figure. The spectra consist of a number of narrow bands typically 10–20 nm in width. This value compares with the 70–80 nm width measured for isolated silver-colloidal particles in aqueous solution. Similar widths of 40–85 nm are observed in the near-field spectra of isolated 20 nm gold particles.[7] The spectra depend markedly on the location above the film at which the near-field tip was parked. At the same time the spectra do not correlate in any discernable manner with the *type* of spot at which they were collected. That is, high spots or interstices do not produce any significant differences in the spectra, such as lower average intensities or different average numbers of bands. Moreover, it is clear that the same spot can be a hot spot or

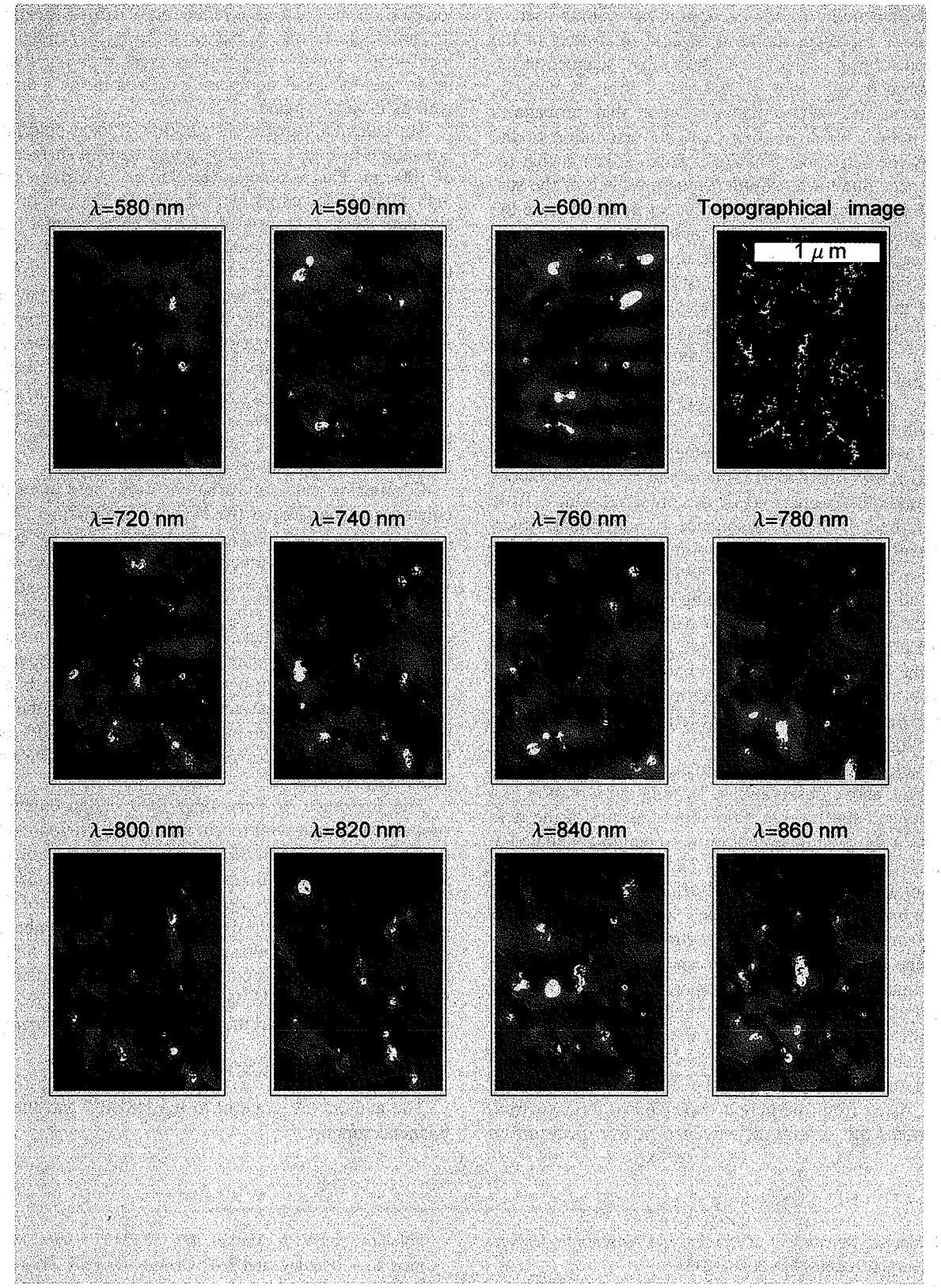

FIG. 4. (Color) Calculated near-field false-color images (i.e., maps of the square modulus of the local electric field) computed on a 10-nm grid, 100 nm above the surface for the various wavelengths indicated. The topographic image of the simulated assembly of silver-colloid clusters used in the computation is shown in the upper right-hand corner. The vertical range in the images is approximately 1100 nm. (The height range measured by the fiber tip in the experimental topographic images shown in Fig. 1 corresponds to approximately 90 nm. This is partly due to the fact that the tip is of finite size and cannot descend into all of the surface interstices.) Note the similarity to the experimentally produced cluster images. Minimum intensity is shown as black, maximum is yellow. The intensity range covers approximately a factor of 4.

a cold zone depending on the excitation wavelength used.

The spectra represent the relative field intensities of the normal modes lying in the wavelength range scanned at the locations probed above the silver surface. More accurately, they represent the electromagnetic wave that propagates down the optical fiber resulting from the excitation of the fiber tip by the self-consistent field, which exists at that location in space due to the simultaneous presence of the surface and the tip excited by the evanescent field. Because the fields are enhanced due to the silver surface, we maintain that the images and the spectra are representative, more or less, of the fields that would have existed at the surface in the absence of the tip, except for the averaging effect due to the tip's finite size, which corresponds to an effective optical aperture of ~50–100 nm. Hence, the more distinct peaks shown in Fig. 2 likely represent spectra of individual normal SP modes, suggesting that, on average, some ten normal modes lie in the 720–840 nm region of the spectrum. To the extent that widths of the better-resolved peaks represent homogeneous linewidths, the lifetime of the SP normal modes of the colloid cluster are ~40 fs, as compared with ~10 fs for the lifetime of the SP resonance of individual silver-colloidal particles in aqueous solution. (The lifetime τ was calculated using the expression $\tau = 2\hbar/\Gamma$, where Γ is the full width at half height.) The lengthening of the lifetime on going from the isolated to the coupled particles can be due to a number of effects, including a change in the resonance condition of the system. The measured bandwidths are also expected to reflect perturbative effects by the tip which, intuitively, are expected to reduce the lifetime. Hence, the 40 fs lifetime is likely a lower limit.

The simulated images and spectra are in substantial agreement with the above observations. Turning our attention first to the simulated spectra, Fig. 3(a) shows spectra of the field intensity as a function of excitation wavelength calculated at two points separated laterally by approximately 580 nm, each 10 nm above a computed self-affine surface containing 2,500 monomers, with approximate lateral dimensions of $1100 \times 600\,\text{nm}^2$. The calculated spectra covering the wavelength range 720 to 950 nm, corresponding to the experiment, qualitatively resemble the experimental spectra. They contain approximately the same number of prominent resonances with widths ~10–20 nm in the range considered.

The calculated dependence of the intensity of the local fields on h, the probe point above the surface, is illustrated in Fig. 3(b). Aside from the height dependence, this spectrum also illustrates the striking dependence of the spectrum on location on the surface, a reflection of strong localization of the hot spots in the xy plane. A strong dependence of the local-field intensity on h is observed implying that, in the near zone, the local fields are localized in the z direction as well as in the xy plane.

The calculated spatial distribution of local-field intensities are shown in Fig. 4 assuming a constant tip-surface distance of 100 nm. This is a somewhat larger tip-surface separation than what is used experimentally. It was chosen, however, to simulate the averaging effect of the experimental tip, which is not a point tip as assumed in the calculations. At this tip-surface distance the calculated intensity excursions from the cold zones to the hot spots are of the order of 4, as observed experimentally. (The effect of averaging affects a number of experimentally observed aspects of the near-field signal. For example, the drop in signal intensity over the first 100 nm or so as the tip is retracted from the surface is less than what is calculated.) The pattern of observed "hot spots" and their strong spectral dependence are very similar to what was observed experimentally (Fig. 1).

Contrasting with the variation in the field intensities calculated 100 nm above the surface (simulating the experiment), the local-field intensities very close to the surface are predicted to be very much more heterogeneous so that the variation in field intensity between the hot spots and the cold zones can exceed 10^5, implying local SERS enhancements in excess of 10^{10} and enhancements of nonlinear optical effects that can be locally enhanced several orders above that. In fact, the observation of near-field nonlinear effects may be a convenient way for measuring the full extent of the variation of the intensity between the hot spots and the cold zones that is less sensitive to the averaging effect due to the finite size of the near-field probe.

The existence of very large-field enhancements at hot spots is consonant with recent reports by Kneipp *et al.*,[4] who report sufficiently high SERS enhancements to allow the observation of SERS from single-adsorbate molecules. The results of this paper provide a rationale for some of those observations in terms of the very large local enhancements possible in the hot spots on illuminated fractal objects. Nie and Emory have also reported very high SERS intensities but from *single* silver-colloidal particles.[16] Hence, their observations are not related to the fractal clusters considered here.

ACKNOWLEDGMENTS

The authors are grateful to the NSERC and the NSF for financial support.

*Present address: Department of Physics and Astronomy, University of Georgia, Athens, GA 30602-2451.

[1] V. A. Markel, L. S. Muratov, M. I. Stockman, and T. F. George, Phys, Rev. B **43**, 8183 (1991); V. M. Shalaev, Phys. Rep. **272**, 61 (1996); V. M. Shalaev, R. Botet, J. Mercer, and E. B. Stechel, Phys. Rev. B **54**, 1 (1996); E. Y. Poliakov, V. M. Shalaev, V. A. Markel, and R. Botet, Opt. Lett. **21**, 1628 (1996); M. I. Stockman, Phys. Rev. E **56**, 6494 (1997); Phys. Rev. Lett. **79**, 4562 (1997).

[2] V. A. Markel, V. M. Shalaev, E. B. Stechel, W. Kim, and R. L. Armstrong, Phys. Rev. B **53**, 2425 (1996); V. M. Shalaev, E. Y. Poliakov, and V. A. Markel, *ibid.* **53**, 2437 (1996); M. I. Stockman, L. N. Pandey, and T. F. George, *ibid.* **53**, 2183 (1996); M. I. Stockman, L. N. Pandey, L. S. Muratov, and T. F. George, *ibid.* **51**, 185 (1995); A. V. Butenko, V. M. Shalaev, and M. I. Stockman, Z. Phys. D **10**, 81 (1988); V. M. Shalaev and M. I. Stockman, *ibid.* **10**, 71 (1988).

[3] J. D. Jackson, *Classical Electromagnetism* (Wiley, New York, 1975); M. Kerker, D. S. Wang, and H. Chew, Appl. Opt. **19**, 4159 (1980); C. Flytzanis, Prog. Opt. **29**, 2539 (1992).

[4] K. Kneipp, Y. Wang, H. Kneipp, L. Itzkan, R. R. Dasari, and M. S. Feld, Phys. Rev. Lett. **76**, 2444 (1996); K. Kneipp, Y. Wang,

H. Kneipp, L. T. Perelman, L. Itzkan, R. R. Dasari, and M. S. Feld, *ibid.* **78**, 1667 (1997).

[5]E. Y. Poliakov, V. A. Markel, V. M. Shalaev, and R. Botet, Phys. Rev. B **57**, 14 901 (1998).

[6]D. P. Tsai, J. Kovacs, Z. Wang, M. Moskovits, V. M. Shalaev, J. Suh, and R. Botet, Phys. Rev. Lett. **72**, 4149 (1994); P. Zhang, T. Haslett, C. Douketis, and M. Moskovits, Phys. Rev. B **57**, 15 513 (1998).

[7]T. Klar, M. Perner, S. Grosse, G. von Plessen, W. Spirkl, and J. Feldmann, Phys. Rev. Lett. **80**, 4249 (1998).

[8]D. P. Tsai, Z. Wang, and M. Moskovits, Proc. SPIE **1855**, 93 (1993); D. P. Tsai, A. Othonos, M. Moskovits, and D. Uttamchandani, Appl. Phys. Lett. **64**, 1768 (1994).

[9]E. Betzig, P. L. Finn, and J. S. Weiner, Appl. Phys. Lett. **60**, 2484 (1992).

[10]B. Vlckovà, X. J. Gu, D. P. Tsai, and M. Moskovits, J. Phys. Chem. **100**, 3169 (1996).

[11]D. Weitz and M. Oliveria, Phys. Rev. Lett. **52**, 1433 (1984); P. Meakin, *ibid.* **51**, 1119 (1983); R. Jullien, M. Kolb, and R. Botet, J. Phys. (France) Lett. **45**, L211 (1984).

[12]S. I. Bozhevolnyi, V. A. Markel, V. Coello, W. Kim, and V. Shalaev, Phys. Rev. B **58**, 11 441 (1998).

[13]R. Jullien and R. Botet, *Aggregation and Fractal Aggregates* (World Scientific, Singapore, 1987).

[14]A. Lakhtakia, J. Mod. Phys. C **3**, 583 (1992).

[15]E. M. Purcell and C. R. Pennypacker, Astrophys. J. **186**, 705 (1973).

[16]S. Nie and S. R. Emory, Science **275**, 1102 (1997).